

Mass Transport Effects on Electroreduction of Carbon Dioxide

Tiek Aun Tan¹, Sara Yasina binti Yusuf¹ and Umi Fazara Muhd Ali¹

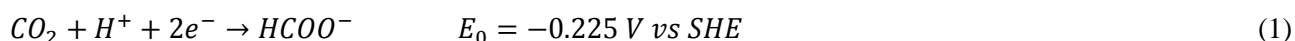
¹Universiti Malaysia Perlis

Abstract: The electrochemical reduction of carbon dioxide (CO_2) into formic acid ($HCOOH$) on a Sn cathode is governed by mass transport. This work investigates the effects of mass transport of CO_2 to a Sn plated electrode on CO_2 reduction. First, a potential of -1.9 V vs SCE is applied to the cathode for two hours at different rotating cathode speeds. It is found that at a rotating speed of 240 rpm, the obtained current density is 70.91 Am^{-2} which increases to 108.67 Am^{-2} at 540 rpm and to 123.47 Am^{-2} at 960 rpm. The samples are analyzed using HPLC and is found to contain $HCOOH$. $HCOOH$ decreases when the rotating speed of cathode is increased. To account for H_2 evolution, cyclic voltammetry is carried out. The catholyte undergoes pre-electrolysis with a Pt cathode and purged with N_2 . The Pt cathode is then replaced with a Sn plated carbon cathode and cyclic voltammetry with a maximum negative potential of -2.5 V vs SCE is carried out on the system to account for H_2 evolution. Then the catholyte is saturated with CO_2 and cyclic voltammetry is repeated on the system. CO_2 reduction is accounted by subtracting the effects of H_2 evolution from the CO_2 cyclic voltammogram. This is done at varying rotating cathode speed at 240 rpm, 540 rpm, and 960 rpm. When the Sn cathode is rotated at 240 rpm, CO_2 reduction initiates at circa -0.7 V vs SHE and the difference in area under the N_2 and CO_2 curve is calculated to be $7.926 \times 10^{-4} \text{ AV}$. When the cathode rotating speed is increased to 540 rpm, the difference in area under the N_2 and CO_2 curve is calculated to be $4.85 \times 10^{-4} \text{ AV}$. When the cathode rotating speed is further increased to 960 rpm, a slight drop is suffered with the difference in area under the N_2 and CO_2 curve calculated to be $4.54 \times 10^{-4} \text{ AV}$. It can be concluded that increasing the mass transport of CO_2 does not necessarily improve reduction performance possibly due to migration of $HCOOH$ to the anode where it is oxidized back into CO_2 and OH^- to the cathode to form H_2O , further reduction of $HCOOH$ into other products, the formation of a Sn- CO_2 complex, and competing reduction of impurities at the cathode.

Keywords: Carbon dioxide, Electroreduction, Electrolyte, Formic acid

1. Introduction

Electrochemical reduction can valorise CO_2 into $HCOOH$ on a Sn cathode (Eq. 1).



$HCOO^-$ requires relatively little energy to form and can be converted with high Faradaic efficiencies [1]. The process first requires $CO_{2(g)}$ or $CO_{2(aq)}$ to be adsorbed onto the Sn electrode. Electricity is used to supply electrons for the reduction process of the $CO_{2(ad)}$ to $CO_{2(ad)}^{\cdot-}$. The radical anion then desorbs into the electrolyte and undergoes protonation to form $HCOO^\cdot$. The $HCOO^\cdot$ radical then receives another electron to form $HCOO^-$ and a H^+ to form $HCOOH$ [2]. This is shown in Eq. 2 to Eq. 7.



The major competing reaction is H_2 evolution from the reduction of H^+ present in the solvent. The H_2 evolution can be written as in Eq. 9 to Eq. 11. [3]



Hori claims that H_{ads} deactivates the $CO_2^{\cdot-}$ radical to CO_{ads} [3].



Chen et.al. reported that H_{ads} reduces the electro-active surface area of the cathode and increase its electrical resistance [4].

This paper presents the findings on the effects of the transport of CO_2 to the cathode.

2. Methodology

A *Sn* plated glassy carbon rotating disc is the cathode, and *Pt* wire is the anode. The electrolyte is H_2O with $KHCO_3$ as supporting electrolyte. The reactor is batch type with separation of the catholyte and anolyte achieved using a Nafion membrane. The selective permeable membrane separating the anode and cathode chambers stops the oxidation of the newly reduced $HCOO^-$ back into CO_2 and the reduction of O_2 into OH^- as shown in Eq. 12 and Eq. 13.



Chrono amperometry, high pressure liquid chromatography and cyclic voltammetry is used to investigate the mass transport effects of CO_2 on CO_2 reduction.

2.1. Chrono Amperometry

Chrono Amperometry is carried out on the system to investigate the current performance of the electrolysis as a function of time at a set potential. Three sets of experiment are carried out where the electrode is rotated at a speed of 240, 540, and 960 rpm respectively. Prior to each set of experiment, the remaining *Sn* will be stripped off first and then re-deposited under the same conditions to ensure the thickness of the *Sn* layer for each set run is similar. A fresh batch of electrolyte is also prepared and purified through pre-electrolysis.

A potential of -1.9 V vs SCE is applied on the cathode for two hours and the current performance is recorded. The potentials were later converted to V vs SHE to account for pH change.

2.2. High Pressure Liquid Chromatography

High Pressure Liquid Chromatography is used to confirm the presence of $HCOOH$. The column is a RP C-18 column provided by Merck and the mobile phase 0.01 M KH_2PO_4 + 5 % methanol acidified to pH 2.7 with H_3PO_4 . The samples were flowed at 1ml/min. $HCOOH$ is detected at 220 nm UV wavelength. The results are compared with a standard curve of a known sample containing 10 % $HCOOH$.

2.3. Cyclic Voltammetry

Cyclic voltammetry is carried out on the system to investigate the current performance of the electrolysis as a function of potential. Three sets of experiment are carried out where the electrode is rotated at a speed of 240, 540, and 960 rpm respectively. Prior to each set of experiment, the remaining *Sn* will be stripped off first and then re-deposited under the same conditions to ensure the thickness of the *Sn* layer for each set run is similar. A fresh batch of electrolyte is also prepared and purified through pre-electrolysis.

A competing reaction, H_2 evolution is unavoidable as it initiates at potentials close to CO_2 reduction. In each set of experiment, to account for current due to H_2 evolution, first the electrolyte is purged with N_2 to remove

CO_2 , then a CV is ran on the sample and the resulting current which initiates at circa -0.7 V vs SHE must be due to H_2 evolving at the cathode. The set up at this point cannot be disturbed as even a slight change in position of any of the electrodes will alter the Ohmic resistance between them. Then CO_2 is reintroduced into the sample and a CV is carried out on the sample. This time, the current initiated at circa -1.5 V vs SCE is due to CO_2 reduction and H_2 evolution. The effect of H_2 evolution is then subtracted out using data from the first CV run.

3. Results

3.1. Chrono Amperogram

A potential of -1.9 V vs SCE is applied on the electrolyte for two hours with varying rotating speeds of 240 rpm, 540 rpm, and 960 rpm.

For reduction of CO_2 at 240 rpm, the theoretical current density is 0.20 Am^{-2} while the obtained current density is 70.91 Am^{-2} . For reduction of CO_2 at 540 rpm, the theoretical current density is 0.30 Am^{-2} while the obtained current density is 108.67 Am^{-2} . For reduction of CO_2 at 960 rpm, the theoretical current density is 0.40 Am^{-2} while the obtained current density is 123.47 Am^{-2} . There are huge discrepancies between the theoretical current density and the obtained current density. The theoretical current density only considers the mass transport limited current for a two electron reduction of the electro-active CO_2 species and does not factor in other current density sources that may be present in the process. In reality, there may be other reactions consuming electrons such as H_2 evolution or reduction of the cation originating from the salt used to improve the conductivity of ultra pure H_2O .

Fig 1 shows the reduction of CO_2 on a Sn cathode rotating at 240 rpm, 540 rpm, and 960 rpm respectively for two hours. When the rotating speed is 240 rpm, the charge passed is 10.01 Q. The Nernst Diffusion Layer is calculated to be $3.21 \times 10^{-5} \text{ m}$. When the rotating speed is increased to 540 rpm, a higher charge is passed being 15.34 Q. Improved mass transport of feedstock to the cathode allows reduction to proceed at a higher rate. The Nernst Diffusion Layer is calculated to be $2.14 \times 10^{-5} \text{ m}$. When the rotating speed is 960 rpm, an even higher charge is passed being 17.42 Q. Improved mass transport of feedstock to the cathode allows reduction to proceed at a higher rate. This does not necessarily mean that CO_2 is being reduced at a higher rate. Referring to Fig 3, background reaction, i.e. H_2 evolution may also proceed at a higher rate. The Nernst Diffusion Layer is calculated to be $1.60 \times 10^{-5} \text{ m}$.

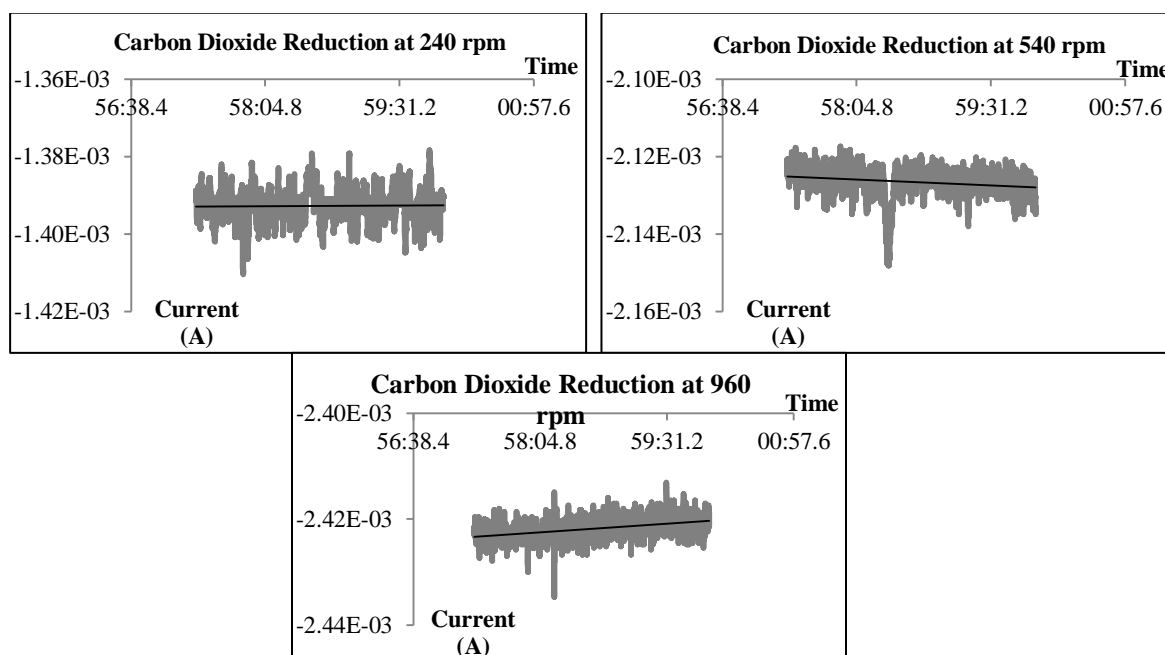


Fig. 1: CO_2 Reduction at 240 rpm, 540 rpm, and 960 rpm respectively for 2 hours.

If the theoretical current density is used to calculate the theoretical amount of $HCOOH$ that is obtained, then the theoretical amount of charge going into the system is then 0.028 Q for CO_2 reduction at 240 rpm, 0.042 Q for CO_2 reduction at 540 rpm and 0.056 Q for CO_2 reduction at 960 rpm. The theoretical amount of $HCOOH$ that can be produced is 6.68×10^{-6} g for CO_2 reduction at 240 rpm which increases to 1.00×10^{-5} g for CO_2 reduction at 540 rpm and to 1.34×10^{-5} g for CO_2 reduction at 960 rpm. The Nernst Potential for CO_2 reduction at 240 rpm is then -0.289 V vs SHE which increases to -0.294 V vs SHE for CO_2 reduction at 540 rpm and to -0.298 V vs SHE for CO_2 reduction at 960 rpm. The Nernst Potential for CO_2 reduction at 240 rpm is then -0.533 V vs SCE which increases to -0.538 V vs SCE for CO_2 reduction at 540 rpm and to -0.542 V vs SCE for CO_2 reduction at 960 rpm.

If the obtained current density is used to calculate the amount of $HCOOH$ that is obtained, then the amount of charge going into the system is then 10.01 Q for CO_2 reduction at 240 rpm, 15.34 Q for CO_2 reduction at 540 rpm and 17.42 Q for CO_2 reduction at 960 rpm. The theoretical amount of $HCOOH$ that can be produced is 2.39×10^{-3} g for CO_2 reduction at 240 rpm which increases to 3.66×10^{-3} for CO_2 reduction at 540 rpm and to 4.15×10^{-3} for CO_2 reduction at 960 rpm. The Nernst Potential for CO_2 reduction at 240 rpm is then -0.366 V vs SHE which increases to -0.371 V vs SHE for CO_2 reduction at 540 rpm and to -0.373 V vs SHE for CO_2 reduction at 960 rpm. The Nernst Potential for CO_2 reduction at 240 rpm is then -0.610 V vs SCE which increases to -0.615 V vs SCE for CO_2 reduction at 540 rpm and to -0.617 V vs SCE for CO_2 reduction at 960 rpm.

This assumes that all charge provided to the system is used to reduce CO_2 into $HCOOH$ at 100% efficiency.

3.2. High Pressure Liquid Chromatograph

A maximum shift of 0.18 min between the standard $HCOOH$ curves and the sample $HCOOH$ curves are observed. However the presence of $HCOOH$ is still confirmed but not quantified due to a difficulty in measuring concentrations of less than 1%. The area under the $HCOOH$ curve is a representation of the quantity of $HCOOH$ produced and is used as a relative measure. It is found that with an increase of rotation speed which provides better mass transport, the area under the $HCOOH$ curve decreases, which meant that less $HCOOH$ is produced. The decrease in area is documented as 301,612 for 240 rpm, to 270,934 for 540 rpm and 231,568 for 960 rpm. Fig 2 shows the $HCOOH$ peak for CO_2 on a Sn cathode rotating at 240 rpm, 540 rpm and 960 rpm for two hours.

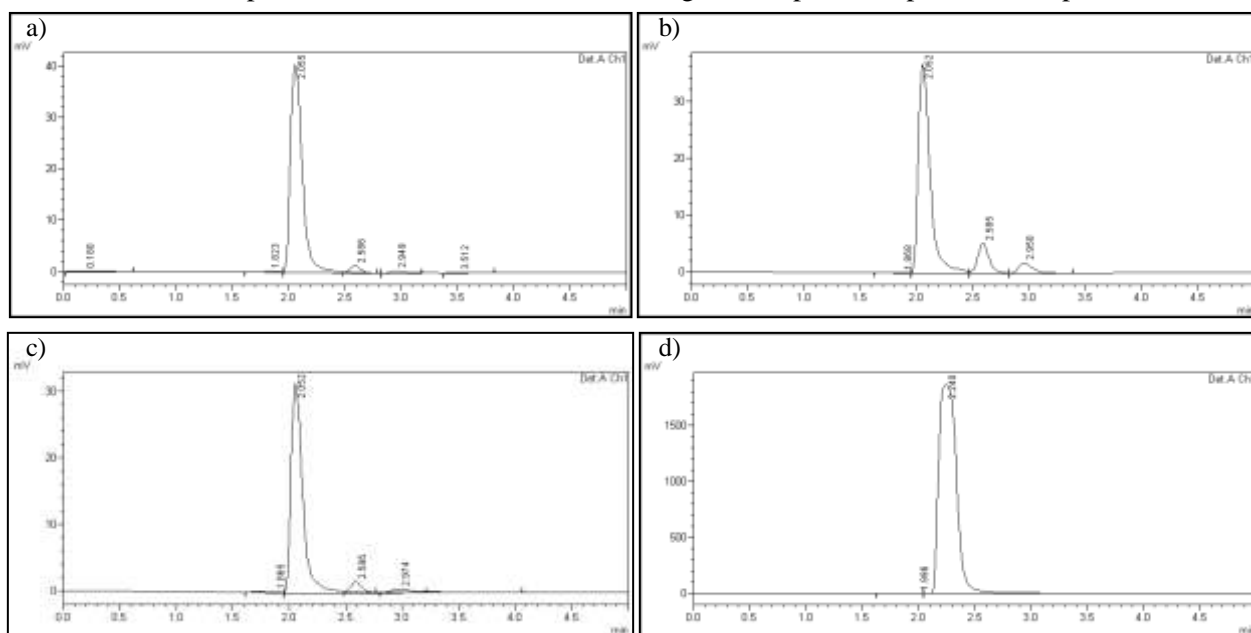


Fig. 2: a) $HCOOH$ peak for CO_2 Reduction at 240 rpm, b) $HCOOH$ peak for CO_2 Reduction at 540 rpm, c) $HCOOH$ peak for CO_2 Reduction at 960 rpm, d) 10% $HCOOH$ peak

3.3. Cyclic Voltammograms

If the forward pass potential sweep is asymmetric as the backward pass, it is likely due to the evolution of H_2 on the electrode surface of the electrode. The H_2 disrupts the current flowing through the system by absorbing on the electrode surface. The degree of asymmetry for the forward and backward pass in the CO_2 reduction sweep is less pronounced than in the H_2 evolution sweep. This suggests that CO_2 is preferentially reduced over H_2 . Hence it might be erroneous to directly subtract the effect of H_2 evolution from the reduction of CO_2 and H_2 because it only represents the worst case scenario, which is H_2 evolution occurring at the maximum without being impeded by the reduction of CO_2 [3]. Only data from the forward pass, the potential sweep from -0.5 V vs SHE to -1.72 V vs SHE is used. These values are still meaningful relative to each other because the degree of impedance caused by H_2 evolution is assumed similar for all runs.

The reduction curve at circa -0.1 V vs SHE is due to part of the Sn reducing into SnO_x [5]. This is beneficial to the process as SnO_x play a bigger role than Sn in the reduction of CO_2 . This reduction process is the same for all runs as its cyclic voltammetric profile is similar for all same type of curve. In the reduction of CO_2 , SnO_x formation always initiates at a less negative potential than for the H_2 evolution run. In the backward pass, there exist a positive current circa -0.1 V vs SHE. The current is the stripping region where SnO_x is oxidised to Sn and Sn into Sn^{2+} [5].

The effects of mass transport were studied by varying the rotating speed of the cathode which in turn governs the transport of CO_2 to the cathode. The initiating potential for CO_2 reduction does not vary significantly for all rotating speeds.

Fig 3 shows the graph of reduction of CO_2 on a Sn cathode rotating at 240 rpm, 540 rpm, and 960 rpm respectively. CO_2 reduction and H_2 evolution initiates at nearly the same potential, circa -1.5 V vs SCE. When the cathode is rotated at 240 rpm, the difference in area under the N_2 and CO_2 curve is calculated to be 7.926×10^{-5} AV. When the cathode rotating speed is increased to 540 rpm, the difference in area under the N_2 and CO_2 curve is calculated to be 4.85×10^{-4} AV. When the cathode rotating speed is further increased to 960 rpm, a slight drop is suffered the difference in area under the N_2 and CO_2 curve is calculated to be 4.54×10^{-4} AV.

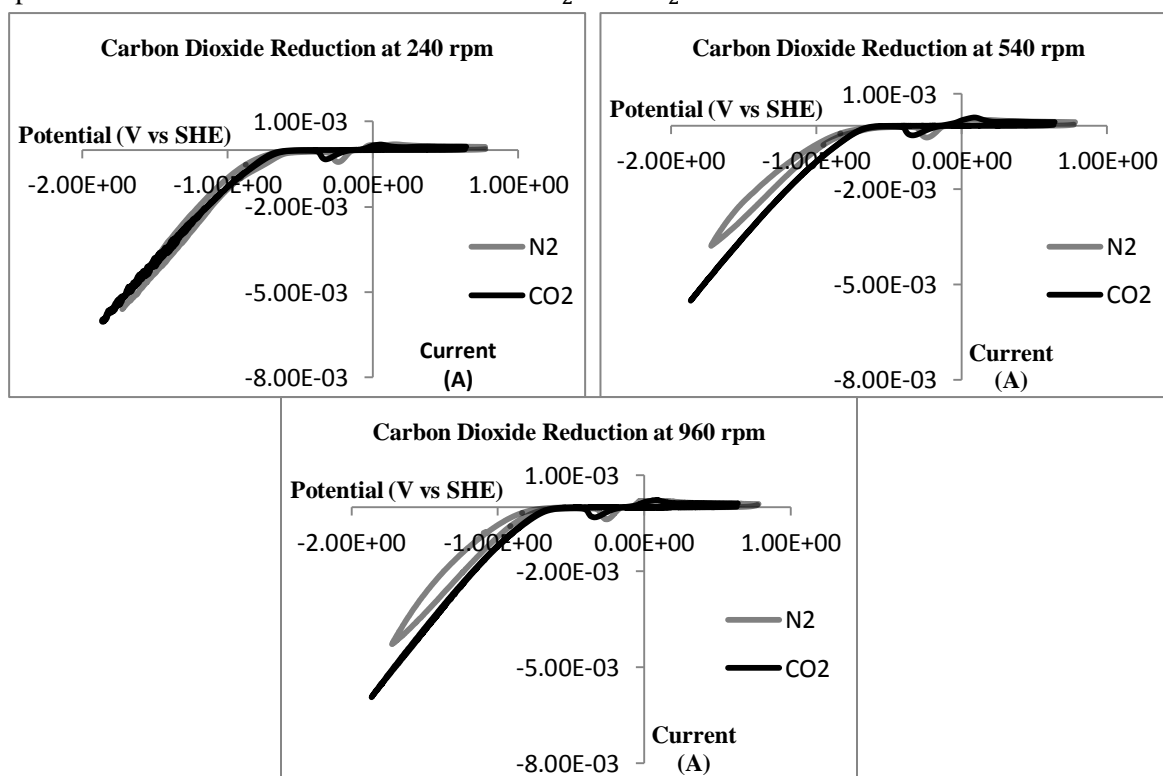


Fig. 3: Cyclic Voltammogram for CO_2 Reduction at 240 rpm, 540 rpm and 960 rpm respectively

3.4. Discussion

Chrono amperogram data shows that with increasing rotating speed, a higher current is passed, meaning that a reduction reaction proceeds more vigorously. High pressure liquid chromatography data shows that the $HCOOH$ decreases with increasing rotating speed. Cyclic voltammetry data shows that the difference in area under the N_2 and CO_2 curve increases drastically from a rotating speed of 240 rpm to 540 rpm, and only drop slightly with an increase to 960 rpm. These may mean a few things; migration of $HCOOH$ to the anode where it is oxidized back into CO_2 and OH^- to the cathode to form H_2O , further reduction of $HCOOH$ into other products, the formation of a $Sn-CO_2$ complex, when the bond between Sn and CO_2 does not always break and the CO_2 carries the Sn into the bulk electrolyte as $Sn-CO_2$, and competing reduction of impurities at the cathode [6]. This effect may be more prominent at high rotating speeds where CO_2 transport to the cathode is improved.

4. Conclusions

When the rotating speed of the Sn cathode is increased, CO_2 mass transport to the cathode increases. This results in a higher current density. The recorded current density for reduction of CO_2 at 240 rpm, 540 rpm, and 960 rpm are 70.91 Am^{-2} , 108.67 Am^{-2} , and 123.47 Am^{-2} respectively. This is however much higher than the calculated theoretical current density which expects 0.20 Am^{-2} , 0.30 Am^{-2} , and 0.40 Am^{-2} respectively. The theoretical current density only considers the mass transport limited current for a two electron reduction of the electro-active CO_2 species and does not factor in other current density sources that may be present in the process. In reality, there may be other reactions consuming electrons meant for the CO_2 reduction. It does not necessarily mean that CO_2 is being reduced at a higher rate. A major competing reaction is H_2 evolution. Cyclic voltammetry is used to study the effects of H_2 evolution. The area under the graph for reduction of CO_2 which can be directly related to the current density, at 240 rpm, 540 rpm, and 960 rpm are $7.926 \times 10^{-5} \text{ AV}$, $4.85 \times 10^{-4} \text{ AV}$, and $4.54 \times 10^{-4} \text{ AV}$ respectively. Other competing reactions may be caused by migration of $HCOOH$ to the anode where it is oxidized back into CO_2 and OH^- to the cathode to form H_2O , further reduction of $HCOOH$ into other products, the formation of a $Sn-CO_2$ complex, when the bond between Sn and CO_2 does not always break and the CO_2 carries the Sn into the bulk electrolyte as $Sn-CO_2$, and competing reduction of impurities at the cathode.

5. Acknowledgement

This work is supported by the Research Acculturation Grant Scheme 9018-00033.

6. References

- [1] A. S. Agarwal. (September 2011). The electrochemical reduction of carbon dioxide to formate/formic acid: engineering and economic feasibility. *Chem. Pub. Soc. [Online]*. 4(12). pp. 1301-1310. Available: <http://onlinelibrary.wiley.com/doi/10.1002/cssc.201100220/abstract>.
- [2] W. Li. "Electrocatalytic reduction of CO_2 to small organic molecule fuels on metal catalysts," in *ACS Symposium Series* 2010, pp. 56-76.
- [3] Y. Hori. (2008). Electrochemical CO_2 reduction on metal electrodes. *Modern Aspects of Electrochemistry*. Springer. pp. 89-188.
http://dx.doi.org/10.1007/978-0-387-49489-0_3
- [4] F. Chen. (April 2012). Study on hydrogen evolution reaction at a graphite electrode in the all-Vanadium Redox Flow Battery. *Int. J. Electrochem. Sci. [Online]*. pp. 3750-3764. Available: <http://www.electrochemsci.org/papers/vol7/7043750.pdf>
- [5] W. Lv. (December 2013). Studies on the faradaic efficiency for electrochemical reduction of carbon dioxide to formate on tin electrode. *Journal of Power Sources*. pp. 276-281.
- [6] H. Li. (April 2005). The electro-reduction of carbon dioxide in a continuous reactor. *Journal of Applied Electrochemistry*. pp. 955-965.
<http://dx.doi.org/10.1007/s10800-005-7173-4>